

TNFRSF13B VARIANTS ACT AS MODIFIERS TO CLINICAL PHENOTYPES IN COMMON VARIABLE IMMUNE DEFICIENCY DISORDERS

TNFRSF13B VARYANTLARI, YAYGIN DEĞİŞKEN İMMÜN YETMEZLİK KLİNİK FENOTİPİNİN DÜZENLENMESİNDE ROL OYNAR

Sinem FIRTINA¹, Aslı KUTLU², Begüm IŞIKGİL³, Medinenur YOZLU⁴, Beyza Nur CEPECİ⁴, Hülya YILMAZ⁵, Yuk Yin NG⁶, Özden HATIRNAZ NG⁷, Ayça KIYKIM⁸, Esra YÜCEL ÖZEK⁹, Elif AYDINER¹⁰, Safa BARIŞ¹⁰, Ahmet Oğuzhan ÖZEN¹⁰, Serdar NEPESOV¹¹, Yıldız ÇAMCIOĞLU⁸, İsmail REİSLİ¹², Muhlis Cem AR⁵, Müge SAYITOĞLU¹³

¹Istanbul University-Cerrahpasa, Cerrahpasa Faculty of Medicine, Department of Medical Genetics, Istanbul, Türkiye

²Istinye University, Engineering and Natural Science Faculty, Department of Molecular Biology and Genetics, Istanbul, Türkiye

³Istinye University, Institute for Graduate Education, Department of Medical Biology and Genetics, Istanbul, Türkiye

⁴Gezbe Technical University, Science Faculty, Department of Molecular Biology and Genetics, Kocaeli, Türkiye

⁵Istanbul University-Cerrahpasa, Cerrahpasa Faculty of Medicine, Department of Internal Medicine, Division Hematology, Istanbul, Türkiye

⁶Bilgi University, Engineering and Natural Science Faculty, Department of Genetics and Bioengineering, Istanbul, Türkiye

⁷Acibadem Mehmet Ali Aydınlar University, Faculty of Medicine, Department of Medical Genetics, Istanbul, Türkiye

⁸Istanbul University-Cerrahpasa, Cerrahpasa Faculty of Medicine, Department of Infectious Diseases, Division Allergy and Clinical Immunology, Istanbul, Türkiye

⁹Istanbul University, Istanbul Faculty of Medicine, Department of Pediatrics, Division Pediatric Allergy and Immunology, Istanbul, Türkiye

¹⁰Marmara University, Faculty of Medicine, Department of Pediatrics, Division Pediatric Allergy and Immunology, Istanbul, Türkiye

¹¹Medical Park Goztepe Hospital, Clinic of Pediatrics, Division of Pediatric Allergy and Immunology, Istanbul, Türkiye

¹²Necmettin Erbakan University, Faculty of Medicine, Department of Pediatrics, Division Pediatric Allergy and Immunology, Istanbul, Türkiye

¹³Istanbul University, Aziz Sancar Institute of Experimental Medicine, Department of Genetics, Istanbul, Türkiye

ORCID ID: S.F. 0000-0002-3370-8545; A.K. 0000-0002-9169-388X; B.I. 0000-0002-7541-4596; M.Y. 0000-0002-3580-7280; B.N.C. 0000-0001-9417-2943; H.Y. 0000-0001-5664-5893; Y.Y.N. 0000-0001-9755-6045; Ö.H.N. 0000-0001-7728-6527; A.K. 0000-0001-5821-3963; E.Y.Ö. 0000-0003-3712-2522; E.A. 0000-0003-4150-5200; S.B. 0000-0002-4730-9422; A.O.Ö. 0000-0002-9065-1901; S.N. 0000-0002-4551-5433; Y.Ç. 0000-0002-4796-6828; İ.R. 0000-0001-8247-6405; M.C.A. 0000-0002-0332-9253; M.S. 0000-0002-8648-213X

Citation/Atf: Firtina S, Kutlu A, Isikligil B, Yozlu M, Cepci BN, Yilmaz H, et al. TNFRSF13B variants act as modifiers to clinical phenotypes in common variable immune deficiency disorders. Journal of Advanced Research in Health Sciences 2023;6(3):210-218. <https://doi.org/10.26650/JARHS2023-1346155>

ABSTRACT

Objective: The TNF receptor gene 13B (*TNFRSF13B*) is a member of the TNF superfamily which is crucial for B cell maturation, plasma cell differentiation, and antibody response. Impaired expression of the *TNFRSF13B* gene is associated with common variable immune deficiency (CVID), autoimmunity, and lymphoproliferation disorders. Besides the disease-causing variants of this gene, its different isoforms are associated with strong and weak *TNFRSF13B* expression that leads to an unbalanced B cell response.

Materials and Methods: The study detected 26 variants (three synonymous, five missenses, eleven UTR, and seven intronic variants) in the *TNFRSF13B* gene by screening 68 CVID patients with targeted next generation sequencing. An integrative bioinformatics approach was utilized to provide a plausible explanation for CVID associations from different perspectives and to investigate the associations from the clinical findings.

Results: Fifty-eight percent (15/26) of the detected variants were altered regulatory elements, such as transcription factor binding, miRNA binding sites, splice site regions or the thermodynamic impact on protein. We observed that patients who suffered from the potential splicing variants had significantly low IgA levels ($p=0.009$), autoimmunity ($p=0.02$) and gastrointestinal findings ($p=0.05$). In addition, the c.*79A>G 3'-UTR variant was found with the low IgA and IgE levels. Thirteen variants found to have at least tenfold increased allele frequencies as compared to global databases indicating that the *TNFRSF13B* variants, which have a potential regulatory effect, are more common in CVID patients.

Conclusions: All findings suggested that these variants may not be the causative variant for the CVID phenotype but the unbalanced *TNFRSF13B* alternative splices could contribute to the pathogenesis of patients independent from the underlying genetic background of CVID.

Keywords: *TNFRSF13B*, *in silico* analysis, CVID, integrated bioinformatics, PID

ÖZ

Amaç: TNF reseptör üst ailesi üyesi 13B (*TNFRSF13B*), B hücre olgunlaşması, plazma hücresi farklılaşması ve antikor yanıtı için kritik olan TNF üst ailesinin bir üyesidir. *TNFRSF13B* geninin bozulmuş ifadesi, yaygın değişken immün yetmezlik (YDIY), otoimmünite ve lenfoproliferasyon bozuklukları ile ilişkilendirilir. Bu genin hastalığa neden olan varyantlarının yanı sıra bazı farklı izoformlarında B hücre yanıtını değiştirdiği gösterilmiştir.

Gereç ve Yöntemler: Bu çalışmada, 68 YDIY hastası yeni nesil dizileme yöntemi ile taranarak *TNFRSF13B* geninde 26 varyant (üç sinonim, beş yanlış anlamlı, on bir UTR ve yedi intronik varyant) saptanmıştır. Tespit edilen varyantlar etkilerine göre biyoinformatik araçlar ile modellenmiş, etkili olduğu gösterilen varyantların klinik bulgular ile ilişkisi araştırılmıştır.

Bulgular: Saptanan varyantların (15/26) %58'i, transkripsiyon faktörü ya da miRNA bağlama bölgeleri, kırılma bölgeleri veya protein üzerinde termodinamik etkisi olabileceği gösterilen varyantlardır. Biyoinformatik olarak kırılma bölgesini değiştirdiği düşünülen varyantlara sahip hastalarda, diğer hastalara göre anlamlı derecede düşük IgA düzeylerinin ($p=0,009$), otoimmünite varlığının ($p=0,02$) ve gastrointestinal bulgular ($p=0,05$) gibi YDIY fenotipinde görülen bulguların olduğunu gözlemledik. Ayrıca c.*79A>G 3'-UTR varyantının düşük IgA ve IgE seviyeleri ile ilişkili olduğu bulunmuştur. Global veritabanlarına kıyasla on üç varyantın en az on kat artmış alel frekanslarına sahip olduğu bulundu. Bu fark potansiyel düzenleyici etkiye sahip *TNFRSF13B* varyantlarının YDIY hastalarında daha yaygın olduğunu göstermektedir.

Sonuçlar: Bu bulgular, *TNFRSF13B*'deki varyantların YDIY fenotipini açıklaması da, kırılma bölgesini değiştirme potansiyeli olan varyantların YDIY'in altında yatan genetik arka plandan bağımsız olarak hastaların patogenezinin katkısında bulunabileceğini göstermiştir.

Anahtar Kelimeler: *TNFRSF13B*, *in silico* analiz, YDIY, entegre biyoinformatik, PID

Corresponding Author/Sorumlu Yazar: Sinem FIRTINA E-mail: snmfirtina@gmail.com

Submitted/Başvuru: 19.08.2023 • **Revision Requested/Revizyon Talebi:** 31.08.2023 • **Last Revision Received/Son Revizyon:** 31.08.2023

• **Accepted/Kabul:** 01.09.2023 • **Published Online/Online Yayın:** 20.10.2023



This work is licensed under Creative Commons Attribution-NonCommercial 4.0 International License

INTRODUCTION

Common variable immune deficiency (CVID) is the one of the most common types of primary immune deficiencies (PID) with a 1:25.000 frequency in adults (1). CVID is characterized by recurrent infections, low levels of immunoglobulins and predisposition to autoimmunity, cancer, and allergy. The genetic etiology of CVID is complicated. Unlike other types of PID, only 20% of CVID patients, mostly familiar cases, have a chance to define the causative genetic variant. This highlights the importance of not only monogenic inheritance but also complex/polygenic inheritance and/or epigenetic factors. The TNF receptor superfamily member 13B (*TNFRSF13B*) gene variant is one of the most well-known CVID associated genes which is detected in up to 10% of all CVID patients (2).

The *TNFRSF13B* encodes the transmembrane activator calcium modulator, and the cyclophilin ligand-calcium modulating ligand (CAML) interactor (TACI) protein that binds *CAML*, *TNFRSF13* (*APRIL*), and *TNFSF13B* (*BAFF*) ligands and activates the NF κ B signaling pathway (3). The *TNFRSF13B* has an important role in the isotype switching of IgM to other immunoglobulins, plasma cell differentiation, survival of memory B cells, and T cell-independent B cell response (4). The *TNFRSF13B* controls the autoreactive antibody production by downregulating the inducible T cell costimulator (ICOS) gene expression on B cells and maintenance of the homeostasis of B cell tolerance by upregulating the apoptosis and increasing the expression of Fas and FasL (5, 6).

The *TNFRSF13B* gene gives rise to three dominant protein-coding splice variants of TNFRSF13B-201 (293 aa), TNFRSF13B-203 (156 aa) and TNFRSF13B-206 (247 aa). Full-length isoform TNFRSF13B-201 contains four domains; two cysteine-rich domains (CRD1, CRD2), a stalk region; and a transmembrane domain, while TNFRSF13B-206 only has one functional CRD domain and TNFRSF13B-203 has a soluble form with no CRD domain. Studies showed that different isoforms of TACI proteins have different functions. While the short isoform of TACI is found in memory B cells and associated with the classical NF κ B signaling activation, the dominant (long) isoform is found in the cell surface of resting B cells and increased expression of the CD19 and IgG (7).

The Biallelic and/or monoallelic *TNFRSF13B* variants are associated with CVID, selective IgA deficiency, lymphoproliferation, and some autoimmunity disorders like systemic lupus erythematosus (SLE). CVID-associated monoallelic variants are characterized by null or dominant-negative effects and cause haploinsufficiency of the *TNFRSF13B* by impaired ligand binding and lack of NF κ B signaling activation (8).

Studies indicated that the *TNFRSF13B* variants act as a modifier gene rather than a causative gene and modifying variants of the *TNFRSF13B* contribute to the clinical phenotype in some patients (9). The Epistatic effects of *TNFRSF13B* variants with other CVID-associated genes like *TCF3* trigger autoimmunity in CVID patients (10). In addition, some specific variants cause the

downregulation of TACI expression, but this is not a complete loss. Autoimmune diseases with this CVID phenotype provides another example of the modifying effects of *TNFRSF13B* variants (11) (Figure 1).

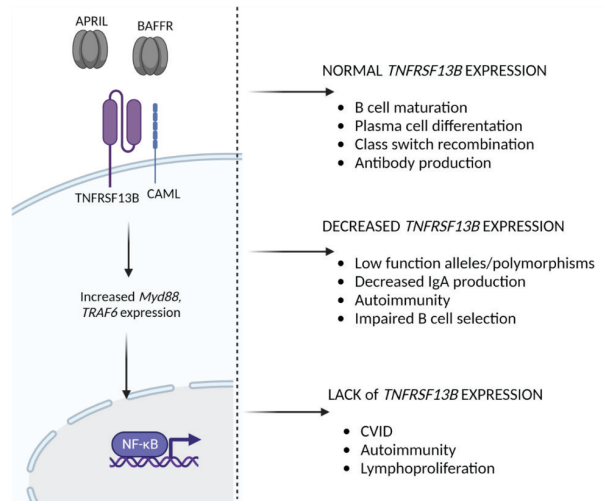


Figure 1: Schematic overview of the *TNFRSF13B* signaling pathway in B-cells and summarize the effects of strong or very *TNFRSF13B* expression in immune response. TNFRSF13B receptor binds to soluble BAFF and/or APRIL ligands and this engagement activates MYD88 and TRAF6 expression. This activation mediates NF κ B signaling pathway

We previously screened disease-causing variants in pediatric primary antibody deficiency (PAD) and severe combined immune deficiency (SCID) and discovered that the genetic background is clearer in SCID patients (12, 13). Due to the genetic heterogeneity of CVID, in this study we aimed to sequence the *TNFRSF13B* gene via next generation sequencing methods in pediatric and adult CVID patients and evaluate the modifying effects of non-disease-causing variants on this clinical phenotype. An integrative informatic analysis was performed to determine potential miRNA and/or transcription factor binding sites for 3-UTR and 5-UTR variants, to evaluate the effects of synonymous variants on RNA folding, to check the presence of splice site effects of missense and synonymous variants, and to reveal any structural and functional impacts of missense variants. We wanted to reveal more about the associations of the *TNFRSF13B* gene variants from different perspectives according to the types of variants.

MATERIAL and METHODS

Screening of *TNFRSF13B* variants

Sixty-eight pediatric and adult CVID patients (twenty-eight females, forty male) were enrolled in this study. The mean age was 20.26 years (min 3-max 68 years), and the mean age of symptom onset was 6.4 years. Forty-three patients were pediatric, and twenty-five patients were adults. Clinical findings

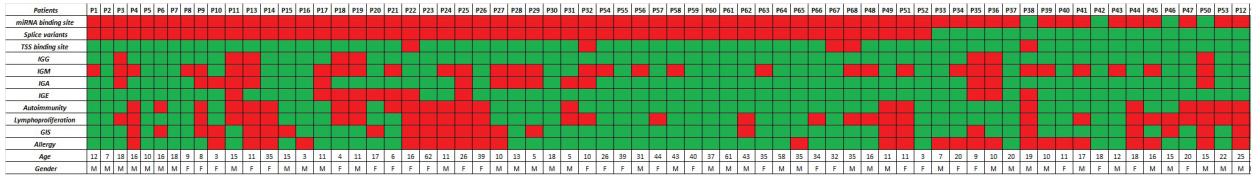


Figure 2: Heat map showing the occurrence of clinical signs and variants in CVID patients. Red boxes indicates that the relevant information is present in the patient. Green boxes indicates that the relevant information is absent in the patient. M: Male F: Female, GIS: Gastrointestinal system, TSS: Transcription start site

are shown in Figure 2. This study was approved by the Ethics Committee of the Cerrahpasa Faculty of Medicine (Date: 01.03.2016, No: A-61). Diagnosis time samples were collected between the years of 2017-2019 and the genomic DNA was extracted using the Qiamp DNA Blood Kit (Qiagen) according to the manufacturer's instructions. Quantification of sequencing libraries was prepared by the Qubit dsDNA HS assay kit (Invitrogen, USA) using the Qubit 4 Fluorometer (Invitrogen, USA). The promoter and the exonic region of the *TNFRSF13B* gene was sequenced by the Illumina Miseq (Illumina USA) sequencer. Quality control parameters and variant analysis were checked by Seq v7.0 (Genomize, Turkey). The *TNFRSF13B* (ENST00000261652.2) variants were filtered and included in the study according to passed filter quality (>Q30) and read depth (>50X) scores. The standard analysis of variant interpretation is given in Figure 3. For further analysis, all variants were checked by several *in silico* prediction tools after categorizing them according to their types. The mirDB, airbase, and TargetScan for 3'-UTR prime variants were used for the determination of *TNFRSF13B* miRNA binding sites; the Human splice finder and Gene Splicer were used for intronic variants

to understand the potential alternative splices; the Missense 3D and Visual Molecular Dynamics (VMD) were used for annotation of missense variants, and the RNA fold (<http://rna.tbi.univie.ac.at/>) was used for checking the effects of synonymous variants to RNA secondary structure and stability (14-20). The Fabian (<https://www.genecascade.org/fabian>) and Regulation Spotter were used for predicting the effects of variants on the transcription factor binding sites (21).

Structural analysis

The full crystal structure of the TAC1 protein was not reported in the literature but the partial crystal structure of the TAC1 protein between residues 68 and 109 was determined by X-Ray (PDB id: 1XU1 / Chain R/S/T) and the NMR (PDB id: 1XUJ/ Chain A) (22). To provide a full understanding, the AlphaFold predicted structure of the TAC1 protein (AF-O14836-F1) was used due to compromising all residues. Prior to analyzing the structural impacts of missense variants, a quality check of the AF-O14836-F1) was performed via the Saves 6.0 tool, compromising five different structure validation tools, e.g., PROCHECK, WHAT_CHECK, ERRAT, VERIFY 3D and PROVE (23-28). To

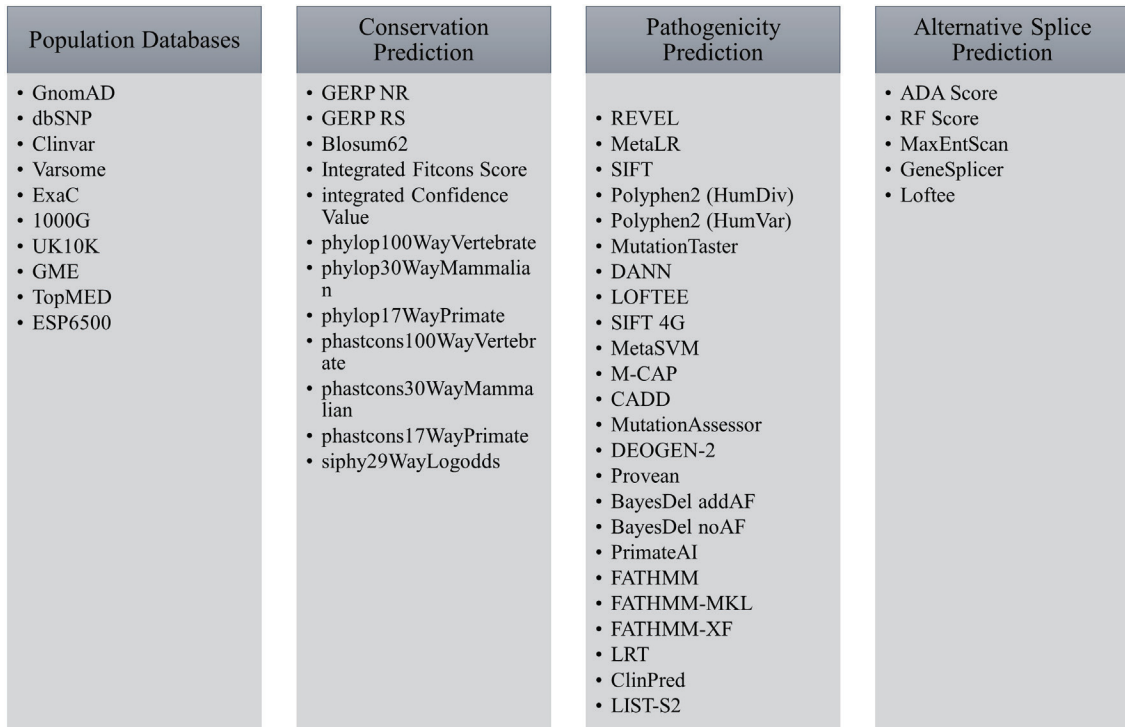


Figure 3: Standard analysis of variant interpretation by Genomize Seq Platform

Table 1: *TNFRSF13B* variants in the patients

Variation Type	Variant *GRCh37	dbSNP	cDNA	AA change	ACMG classification	VAF (in house/global)	VAF fold change	Predicted regulatory effect
3 Prime UTR	17:16842688C>T	rs56153623	c.*173G>A	N/A	B	0.4397 / 0.2482	2 +	miRNA binding site
3 Prime UTR	17:16842774CAT>C	rs150068036	c.*86_*88delITG	N/A	VUS	0.0357 / 0.0557	0.6 -	miRNA binding site
3 Prime UTR	17:16842782T>C	rs1183784784	c.*79A>G	N/A	VUS	0.01 / 0.001	10 +	miRNA binding site
3 Prime UTR	17:16842602G>GCCTCTCT	rs1378399485	c.*252_*259dupCCCTCTCTG	N/A	VUS	0.0129 / 0.0007	18.5 +	miRNA binding site
3 Prime UTR	17:16842661G>C	rs373632897	c.*200C>G	N/A	VUS	0.1379 / 0.0060	23 +	miRNA binding site
3 Prime UTR	17:16842645G>C	rs1597655978	c.*216C>G	N/A	VUS	0.1940 / 0.0070	28 +	miRNA binding site
3 Prime UTR	17:16842777A>C	rs1375454146	c.*84T>G	N/A	VUS	0.0202 / 0.0003	67 +	miRNA binding site
3 Prime UTR	17:16842796A>C	rs1337965516	c.*65T>G	N/A	VUS	0.4343 / 0.0054	80 +	miRNA binding site, splice medium loss donor
3 Prime UTR	17:16842447C>A	rs55701306	c.*414G>A	N/A	B	0.1625 / 0.0817	2 +	No change
3 Prime UTR	17:16842824A>C	rs188626884	c.*37T>G	N/A	VUS	0.0167 / 0.0002	83.5 +	No change
5 Prime UTR	17:16875407A>C	rs1478747037	c.-18T>G	N/A	VUS	0.0156 / 0.0001	156 +	TSS binding site
Intronic	17:16843171A>G	rs11652811	c.632-60T>C	N/A	B	0.1125 / 0.2416	0.4656 -	No change
Intronic	17:16852027T>C	rs2274892	c.445+25A>C	N/A	B	0.4697 / 0.4400	1 +	No change
Intronic	17:16852367G>A	rs537951875	c.200-70C>T	N/A	VUS	0.0619 / 0.0028	22 +	No change
Intronic	17:16852377G>A	rs1397554467	c.200-80C>T	N/A	VUS	0.0177 / 0.0002	88 +	No change
Intronic	17:16852388TA>T	rs67234667	c.200-83del	N/A	VUS	0.1549 / 0.0165	9 +	No change
Intronic	17:16852410G>A	rs1459501406	c.200-113C>T	N/A	VUS	0.0275 / 0.0003	91 +	No change
Intronic	17:16875264G>A	rs1359249090	c.61+65C>T	N/A	VUS	0.0042 / 0.00007	60 +	TSS binding site
Missense	17:16778660A>C	NA	c.44T>G	V15G	VUS	0.0147 / NA		ESE/ESS splice
Missense	17:16842991G>A	rs34562254	c.752C>T	P251L	B	0.1667 / 0.1454	1.146 -	Thermodynamic impact
Missense	17:16852133G>A	rs201124889	c.364C>T	R122W	LB	0.0140 / 0.0003	46 +	Thermodynamic impact
Missense	17:16778693A>C	NA	c.11T>G	L4R	VUS	0.0041 / NA		No change
Missense	17:16843084A>G	rs56063729	c.659T>C	V220A	LB	0.0109 / 0.0101	1.079 -	Splice medium loss donor
Synonymous	17:16855878C>T	rs8072293	c.81G>A	T27=	B	0.6891 / 0.7270	0.9478 +	New Acceptor splice site
Synonymous	17:16842912A>C	rs11078355	c.831T>C	S277=	B	0.5875 / 0.4981	1 +	No change
Synonymous	17:16852206A>C	rs35062843	c.291T>G	P51=	LB	0.0160 / 0.0392	0.408 +	No change

AA: Amino acid, VAF: Variant allele frequency, VUS: Variant of Unknown Significance, LB: Likely Benign, B: Benign, ACMG: The American College of Medical Genetics and Genomics variant classification, ESS: Exonic splicing silencers, ESE: Exonic splicing enhancers, N/A: Not Available

create and visualize mutant TACI protein structures, the Visual Molecular Dynamics (VMD) tool was used to assess the changes in intramolecular interactions, the salt bridge interactions with 3.2 Å oxygen-nitrogen distance cut-off distance were also calculated by VMD. The PremPS and Cupsat tools were used to assess the effects of missense variants on thermodynamic stability by performing Ala-scanning and calculating changes in destabilization tendencies (29, 30). The Stride web tool was used to track changes in the secondary structure between the native and mutant forms (31).

Statistical analysis

Clinical findings between patients with or without the *TNFRSF13B* variants were statistically compared by Pearson's χ^2 or Fisher's exact and $p < 0.05$ was considered as statistically significant. We evaluated the correlation between the *TNFRSF13B* variants and the clinical characteristics such as gender (male vs female), Lymphocyte count (>50000 vs <50000), B lymphocyte percentage ($<20\%$ vs $>20\%$), immunoglobulin levels (normal vs decreased age-dependent IgG, IgM, IgG and IgA levels), autoimmunity (presence vs absence), lymphoproliferation (presence vs absence), allergy (presence vs absence), and gastrointestinal findings (presence vs absence) (32). All statistical analyses were done by the IBM SPSS statistics 20 (IBM Corp. Armonk, NY, USA).

RESULTS

We screened the *TNFRSF13B* variants in sixty-eight CVID patients via next-generation panel sequencing and found twenty-six monoallelic variants. No pathogenic or likely pathogenic variants were detected. Seven variants were classified as benign, three were likely benign and sixteen variants were classified as a variant of unknown significance (VUS) according to ACMG classification criteria. There were ten variants consisting of 3-UTR and one 5-UTR variants, eight coding sequence (three synonymous, five missense) variants, and seven intronic variants. The detailed information about detected variants is provided in Table 1.

We observed increased minor allele frequencies in several variants as compared to The Genome Aggregation Database (gnomAD) and the Exome Sequencing Project (ExAC) population frequency databases. One likely benign and twelve VUS variants were found to have at least tenfold increased allele frequencies when compared to the global databases (Table 1).

Impact of missense variants

Out of twenty-six variants, we reported five missenses; L4R, V15G, R122W, P251L, and V220A. We performed visualization of the TACI protein structure by displaying the locations of all missense variants according to the CRD1 and CRD2 domains and checked the presence of salt bridge interactions in native and mutant TACI protein complexes, but we reported neither the formation of new salt bridge interactions nor the loss of existing ones (Figure 4).

Secondly, we evaluated the thermodynamic changes in our missense variants and found that only the P251L replacement caused a decrease in the destabilization tendency (-0.38 kcal/

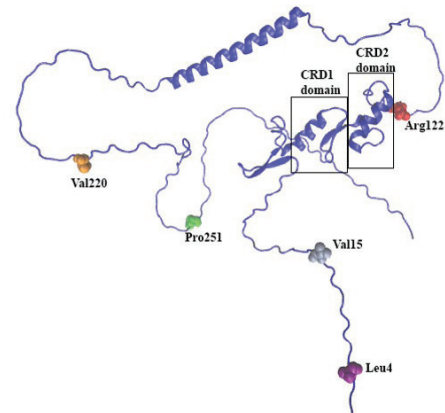


Figure 4: The locations of detected missense variants in 3D TACI protein structure (AlphaFold ID: AF-O14836-F1) CRD: cysteine-rich domains

Table 2: The change in destabilization tendencies upon the presence of missense mutations via PremPs and CUPSAT tools

Variants	PRemPs tool mutation analysis $\Delta\Delta G$ (kcal/mole)	PRemPs tool Ala-scanning $\Delta\Delta G$ (kcal/mole)	CUPSAT tool mutation analysis $\Delta\Delta G$ (kcal/mole)
L4R	0.27	0.32	2.53
V15G	0.31	0.36	0.77
R122W	0.31	0.54	-3.41
V220A	0.28	0.28	0.44
P251L	-0.38	0.20	-1.74

mole) out of the five missense variants. To assess the impact of variants from thermodynamic points of view, Ala-Scanning and destabilization tendencies calculations were performed. Based on the Ala-scanning results by the PremPs tool, we determined that only the R122W and P251L variants were favorably reported to contribute to torsion (Table 2).

Besides evaluating the structural and thermodynamic changes of missense variants, we also identified the splice site effects of the missense variants and determined that the V15G variant was predicted as changing the exon splicing enhancer/silencer (ESE/ESS) site and the V174A variant caused the loss of donor site (score 5.5).

Regulatory effects of UTR variants

To understand the effects of 3-UTR variants, we described the potential miRNA-binding sites on the 3-UTR prime of the *TNFRSF13B* gene using the TargetScan 7.1. tool. Candidate miRNAs were chosen if the predicted context++ score percentile was higher than 95%. We investigated eight of ten 3-UTR variants (c.*65T>G, c.*79A>G, c.*84T>G, c.*86_*88delTG, c.*173G>A,

Table 3: Detailed information about *TNFRSF13B* variants and miRNA target pairing in the seed regions.

Variants	miRNA	Predicted position of target region (bp)	Alignment	Context++ score	Context++ score percentile
c.*65T>G	hsa-miR-1224-3p	62-68	5' ...GGGAGAGAGAAAGAGAGGUGGGG... 3' GACUCCUCUCUCC---UCCACCCC 	-0.33	97
c.*79A>G	hsa-miR-7110-3p	76-83	5' ...GAGGUGGGGAGAGGGGAGAGAGA... 3' GACGUCCCUUACCCUCUCUCU 	-0.61	99
c.*79A>G	hsa-miR-6873-3p	77-83	5' ...AGGUGGGGAGAGGGG-AGAGAGAU... 3' GACUCUCUCUUUCUGUCUCUCUU 	-0.38	98
c.*79A>G c.*84T>G	hsa-miR-3675-3p	79-85	5' ...GUGGGGAGAGGGGAGAGAGAU... 3' AACCCCUCAAGGAA-UCUCUAC 	-0.26	98
c.*86_*88delTG	hsa-miR-4279	87-93	5' ...AGGGGAGAGAGAUAGAGAGAG... 3' CUUCGGCCCUCCUCUC 	-0.33	98
c.*173G>A	hsa-miR-2276-5p	168-174	5' ...AGAGGGAGAGAGACAGAGGGG... 3' GCAGACGUUCCACUGUCUCCCG 	-0.26	97
c.*173G>A	hsa-miR-6826-3p	170-177	5' ...AGGGAGAGAGACAGAGGGGAA... 3' GACUUGUCCUUUCUCUCCCCUC 	-0.55	99
c.*173G>A	hsa-miR-6795-3p	170-176	5' ...AGGGAGAGAGACAGAGGGGAA... 3' GACCCCUUCUUUGCUCCCA 	-0.31	98
c.*200C>G	hsa-miR-2682-3p	194-201	5' ...AGAGGCAGAGAGGAAAGAGGCA... 3' CCUUCUGUCGCGAC--UUCUCCGC 	-0.50	99
c.*200C>G	hsa-miR-6781-3p	194-201	5' ...AGAGGCAGAGAGGAAAGAGGCA... 3' GACUCCGGCACCUU--UUCUCCGU 	-0.48	99
c.*200C>G	hsa-miR-5001-3p	197-203	5' ...GGCAGAGAGGAAAGAGGCAGAG... 3' UUCUUGGACCUUCUCCGUCUU 	-0.26	95
c.*216C>G	hsa-miR-6895-3p	211-217	5' ...GAGGCAGAGAAGGAA-AGAGACAG... 3' GAUUCGGUUCGCGUCUCUGU 	-0.39	98
c.*216C>G	hsa-miR-593-3p	211-217	5' ...GAGGCAGAGAAGGAAAGAGACAG... 3' UCUUUGGGGUCGUCUCUGU 	-0.36	98
c.*216C>G	hsa-miR-6818-3p	211-217	5' ...GAGGCAGAGAAGGAA--AGAGACAG... 3' GACACACUCCUUGUUCUCUGUU 	-0.27	96
c.*216C>G	hsa-miR-5699-3p	213-219	5' ...GGCAGAGAAGGAAAGAGACAGGC... 3' CGAGGUUGUUCUU--UCUGUCCU 	-0.35	97
c.*216C>G	hsa-miR-214-5p	214-221	5' ...GCAGAGAAGGAAAGAGACAGGCA... 3' CGUGUCGUUCACAU--CUGUCCGU 	-0.56	99
c.*216C>G	hsa-miR-6514-3p	215-221	5' ...CAGAGAAGGAAAGAGACAGGCAG... 3' GACCUCACCUUCU--UGUCCGUC 	-0.26	97
c.*252_*259dupCCCTCTCTG	hsa-miR-6769b-3p	253-259	5' ...GAGAGGGAGAGAGGCAGAGAGGG... 3' GAUACCCACCCUGUCUCUCCC 	-0.27	96
c.*252_*259dupCCCTCTCTG	hsa-miR-4723-3p	253-259	5' ...GAGAGGGAGAGAGGCAGAGAGGG... 3' AAACCCUCCUCGG-UCUCUCCC 	-0.31	96
c.*252_*259dupCCCTCTCTG	hsa-miR-3183	253-259	5' ...GAGAGGGAGAGAGGCAGAGAGGG... 3' AGGCUCGUCGAGGCUCUCUCCG 	-0.22	96
c.*252_*259dupCCCTCTCTG	hsa-miR-6892-3p	254-261	5' ...AGAGGGAGAGAGGCAGAGAGGGA... 3' GACGUUCCCAACCCUCUCCU 	-0.59	99
c.*252_*259dupCCCTCTCTG	hsa-miR-4469	256-263	5' ...AGGGAGAGAGGCAGAGAGGGAGA... 3' AGGCUCGUGGGAUUCCUCG 	-0.45	99

c.*200C>G, c.*216C>G and c.*252_*259dupCCCTCTCTG) which were located on a potential miRNA binding site of 22 different miRNAs (Table 3).

In addition, we predicted the impact of our variants on the known transcription factor (TF) binding site by the Fabian (ePOSSUM2) tool and found that the c.-18T>G and c.61+65C>T variants were located on the known TF binding site of the *TNFRSF13B* gene. The c.-18T>G is located in the promoter region of the *TNFRSF13B* and leads to a potential gain in the binding ability *EGR1* and the loss of the *POU2F2* transcription factor. This variant was seen in only four allele in the global databases (C=0.000015 (4/264690, TOPMED), C=0.00000 (0/14050, ALFA)). In our unit, we detected this variant in three of our patients (MAF=0.01). Secondly, a previously known intronic variant (c.61+65C>T) was found in one individual, which caused a potential loss of the *EGR1* binding region, and led to the enhancement of the *POU2F2* binding ability on the *TNFRSF13B* gene.

In silico analysis of synonymous variants

For the next step of this study, we evaluated the possible effects of three synonymous variants (S277S, T27T, and P51P) on the secondary structure of RNA by calculating the changes in minimum free energy (MFE) value. Based on this calculation, we reported almost no change in all replacements; 2% in S277S, 0.7% in T27T, and 1.2% in P51P as compared to native. These little changes suggested that there is no significant change in the secondary structure of RNA in terms of altering binding dynamics. Lastly, we evaluated the alterations on the splice site region, and only reported the T27T variant as a cause of possible activation of the cryptic acceptor site (HSF 56.45%).

Clinical significance of *TNFRSF13B* variants

In order to understand the effects of variants, the relationship between clinical findings and variants was evaluated by statistical analysis. Variants were evaluated both individually and by classifying them according to their types; 'splice effects', 'UTR site', 'TSS binding site', 'miRNA binding site' and 'prior' variants which were VUS classified, increased (>20 times) *in house* allele frequency and have at least one potential effect (c.*65T>G, c.-18T>G, c.61+65C>T and c.364C>T).

We observed that patients who suffered from potential splicing variants (c.44T>G; V15G, c.659T>C; V220A, c.81G>A; T27T, c.*65T>G; n=35) had significantly low IgA levels ($p=0.009$), autoimmunity ($p=0.02$) and gastrointestinal findings ($p=0.05$). In addition, the c.*79A>G 3 prime UTR variant (n=19) that was associated with low IgA ($p=0.05$) and IgE levels ($p=0.007$). c.752C>T (P251L, n=8) was also associated with significantly low IgG levels ($p=0.04$). However, no other clinical correlation was found between other variant types and clinical findings. A heat map showing the occurrence of clinical signs and variants in CVID patients is presented in Table 3.

DISCUSSION

The *TNFRSF13B* gene regulates T-cell-dependent B lymphocyte signaling, antibody production, and plasma cell differentiation by activating the NF κ B pathway (8). Besides this classical

way, the *TNFRSF13B* receptor also promotes immunoglobulin production by interacting with Toll-Like Receptors (TLRs) in B cells (33). Studies showed that monoallelic variants of the *TNFRSF13B* gene were mostly sporadic and characterized by incomplete penetrance and lack of segregation which leads to low-IgA levels, lymphoproliferation, autoimmunity and dysregulated immune response (34).

In this study, we detected twenty-six monoallelic *TNFRSF13B* variants classified as B, LB, or VUS in sixty-eight CVID patients. Within the scope of this paper, we explained the disease associations of twenty-six variants existing in the *TNFRSF13B* gene related to CVID. According to the types of variants, we questioned their possible associations from different perspectives, e.g., missense variants from the structural and thermodynamical point of view, UTR variants from regulatory issues, synonymous variants in RNA binding perspectives and checked out the correlation of these variants with clinical features.

Within the scope of this research no patient was diagnosed with a TACI deficiency but *in silico* analysis of the variants showed that 58% (15/26) have at least one potential regulatory effect on TACI protein. In addition, thirteen variants were found to have at least ten-fold increased allele frequencies when compared to global databases. These high-frequent variants were categorized as VUS classification except for one likely benign R122W missense variant, and 69% of these variants (9/13) could have a potential effect on TACI protein. Based on these results, we indicated that the *TNFRSF13B* variants, which are thought to have a modifying effect on protein, are more common in CVID patients.

Then we evaluated the potential splice site effects of missense, intronic and synonymous *TNFRSF13B* variants and found that the V15G, T27T, V220A and c.*65T>G variants have a potential splice site effect. These variants were also associated with significantly low level IgA, autoimmunity, and GIS findings. In view of the fact of the importance of *TNFRSF13B* splice variants on its function, this data indicates that the alternative splice effects could change the ratio of long/short isoform of the *TNFRSF13B* gene. Unbalanced *TNFRSF13B* alternative splices might contribute to the pathogenesis of patients independent from underlying genetic background of CVID. Evaluating the ratio of the long/short isoform of the *TNFRSF13B* gene on patients might be helpful for understanding the balance of alternative isoforms of TACI and their function.

Additionally, we showed the impact of UTR variants and found two variants (c.-18T>G and c.61+65C>T variants), that are located in known TF binding sites, which might affect the binding ability of *EGR1* and *POU2F2* TFs according to the *in silico* analysis. We did not detect any association between these two variants and clinical findings, but we showed that the 3-prime UTR c.*79A>G (rs1183784784) variant was associated with low IgA and IgE levels. This UTR variant had 10-fold increased allele frequency when compared to the global databases in our research. GWAS studies showed that UTR primer variants of the *TNFRSF13B* gene are associated with low IgG levels (35). Moreover, the P251L variant was also associated with low IgG

levels. Speletas et al. previously showed that patients who suffered from this variant, had increased risk of recurrent infections (36). We showed the association between regulatory variants and immunoglobulin levels that may be helpful to understand the mechanism of modified *TNFRSF13B* variants in primary immunodeficiency.

Even though all these findings covered the possible impacts of detected variants on TAC1 deficiency from different perspectives, the most important limitation of our study is the lack of experimental studies conducted to reveal the changes in mRNA and protein expression levels.

The fact that patients who are not diagnosed with TAC1 deficiency but have potential splice site variants in the *TNFRSF13B* gene have lower IgA and autoimmunity findings, suggesting the potential effect of these variants on TAC1 protein. This study discussed that *TNFRSF13B* gene variants do not cause CVID but it does not explain the phenotype of the disease that may be associated with minimal or moderate regulatory effects and which could accompany the pathogenesis of the disease. Here, it is important to emphasize that even though all this provided information is not sufficient to explain the whole etiology of TAC1 deficiency, it points out the importance of focusing on variants having minimal/moderate regulatory impacts since they were seen more frequently in CVID patients within this study.

Acknowledgements: We would like to thank to Dr. Ozkan Ozdemir for his interpretation for creating a graphical figure 1 with Biorender program.

Ethics Committee Approval: This study was approved by Cerrahpasa Faculty of Medicine Clinical Research Ethics Committee (Date: 01.03.2016, No: A-61).

Peer Review: Externally peer-reviewed.

Author Contributions: Conception/Design of Study- S.F., A.K.; Data Acquisition- H.Y., Y.Y.N., Ö.H.N., A.K., E.Y.Ö., E.A., S.B., A.O.Ö., S.N., Y.Ç., İ.R., B.N.C., M.Y.; Data Analysis/Interpretation- S.F., A.K.; Drafting Manuscript- S.F., A.K.; Critical Revision of Manuscript- M.S., M.C.A.; Final Approval and Accountability- S.F.; Material and Technical Support- S.F., A.K., B.İ.; Supervision- M.S., M.C.A.

Conflict of Interest: The authors have no conflict of interest to declare.

Financial Disclosure: This project was supported by Istanbul University-Cerrahpasa Research Fund (Project no: TYO-2017-24271).

REFERENCES

1. Fried AJ, Bonilla FA. Pathogenesis, diagnosis, and management of primary antibody deficiencies and infections. *Clin Microbiol Rev* 2009;22(3):396-414.
2. Karaca NE, Severcan EU, Guven B, Azarsiz E, Aksu G, Kutukculer N. *TNFRSF13B/TAC1* Alterations in Turkish Patients with Common

- Variable Immunodeficiency and IgA Deficiency. *Avicenna J Med Biotechnol* 2018;10(3):192-5.
3. Wu Y, Bressette D, Carrell JA, Kaufman T, Feng P, Taylor K, et al. Tumor necrosis factor (TNF) receptor superfamily member TAC1 is a high affinity receptor for TNF family members APRIL and BLyS. *J Biol Chem* 2000;275(45):35478-85.
4. Salzer U, Jennings S, Grimbacher B. To switch or not to switch--the opposing roles of TAC1 in terminal B cell differentiation. *Eur J Immunol* 2007;37(1):17-20.
5. Ou X, Xu S, Lam KP. Deficiency in *TNFRSF13B* (TAC1) expands T-follicular helper and germinal center B cells via increased ICOS-ligand expression but impairs plasma cell survival. *Proc Natl Acad Sci U S A* 2012;109(38):15401-6.
6. Figgitt WA, Fairfax K, Vincent FB, Le Page MA, Katik I, Deliyanti D, et al. The TAC1 receptor regulates T-cell-independent marginal zone B cell responses through innate activation-induced cell death. *Immunity* 2013;39(3):573-83.
7. Salzer U, Grimbacher B. TAC1 deficiency - a complex system out of balance. *Curr Opin Immunol* 2021;71:81-8.
8. He B, Santamaria R, Xu W, Cols M, Chen K, Puga I, et al. The transmembrane activator TAC1 triggers immunoglobulin class switching by activating B cells through the adaptor MyD88. *Nat Immunol* 2010;11(9):836-45.
9. Bogaert DJ, Dullaers M, Lambrecht BN, Vermaelen KY, De Baere E, Haerynck F. Genes associated with common variable immunodeficiency: one diagnosis to rule them all? *J Med Genet* 2016;53(9):575-90.
10. Ameratunga R, Koopmans W, Woon ST, Leung E, Lehnert K, Slade CA, et al. Epistatic interactions between mutations of TAC1 (*TNFRSF13B*) and TCF3 result in a severe primary immunodeficiency disorder and systemic lupus erythematosus. *Clin Transl Immunology* 2017;6(10):159-65.
11. Platt JL, de Mattos Barbosa MG, Huynh D, Lefferts AR, Katta J, Kharas C, et al. *TNFRSF13B* polymorphisms counter microbial adaptation to enteric IgA. *JCI Insight* 2021;(6):14-7.
12. Firtina S, Ng YY, Ng OH, Kiykim A, Ozek EY, Kara M, et al. Primary antibody deficiencies in Turkey: molecular and clinical aspects. *Immunol Res* 2022;70(1):44-55.
13. Firtina S, Yin Ng Y, Hatirnaz Ng O, Kiykim A, Aydinler E, Nepesov S, et al. Mutational landscape of severe combined immunodeficiency patients from Turkey. *Int J Immunogenet* 2020;47(6):529-38.
14. Chen Y, Wang X. miRDB: an online database for prediction of functional microRNA targets. *Nucleic Acids Res* 2020;48(1):127-31.
15. Kozomara A, Birgaoanu M, and Griffiths-Jones S. miRBase: from microRNA sequences to function. *Nucleic Acids Res* 2019;47(1):155-62.
16. Agarwal V, Bell GW, Nam JW, Bartel DP. Predicting effective microRNA target sites in mammalian mRNAs. *Elife* 2015;(4):1-3.
17. Desmet FO, Hamroun D, Lalande M, Collod-Beroud G, Claustres M, Beroud C. Human Splicing Finder: an online bioinformatics tool to predict splicing signals. *Nucleic Acids Res* 2009;37(9):67-70.
18. Pertea M, Lin X, Salzberg SL. GeneSplicer: a new computational method for splice site prediction. *Nucleic Acids Res* 2001;29(5):1185-90.
19. Ittisoponpisan S, Islam SA, Khanna T, Alhuzimi E, David A, Sternberg MJE. Can Predicted Protein 3D Structures Provide Reliable Insights into whether Missense Variants Are Disease Associated? *J Mol Biol*

- 2019;431(11):2197-212.
20. Humphrey W, Dalke A, Schulten K. VMD: visual molecular dynamics. *J Mol Graph* 1996;14(1):27-33.
 21. Schwarz JM, Hombach D, Kohler S, Cooper DN, Schuelke M, Seelow D. RegulationSpotter: annotation and interpretation of extratranscriptic DNA variants. *Nucleic Acids Res* 2019;47(1):106-13.
 22. Hymowitz SG, Patel DR, Wallweber HJ, Runyon S, Yan M, Yin J, et al. Structures of APRIL-receptor complexes: like BCMA, TACI employs only a single cysteine-rich domain for high affinity ligand binding. *J Biol Chem* 2005;280(8):7218-27.
 23. Colovos C, Yeates TO. Verification of protein structures: patterns of nonbonded atomic interactions. *Protein Sci* 1993;2(9):1511-9.
 24. Bowie JU, Luthy R, Eisenberg D. A method to identify protein sequences that fold into a known three-dimensional structure. *Science* 1991;253(5016):164-70.
 25. Luthy R, Bowie JU, Eisenberg D. Assessment of protein models with three-dimensional profiles. *Nature* 1992;356(6364):83-5.
 26. Pontius J, Richelle J, Wodak SJ. Deviations from standard atomic volumes as a quality measure for protein crystal structures. *J Mol Biol* 1996;264(1):121-36.
 27. Laskowski RA, Rullmann JA, MacArthur MW, Kaptein R, Thornton JM. AQUA and PROCHECK-NMR: programs for checking the quality of protein structures solved by NMR. *J Biomol NMR* 1996;8(4):477-86.
 28. Hooft RW, Vriend G, Sander C, and Abola EE. Errors in protein structures. *Nature* 1996;381(6):272-6.
 29. Parthiban V, Gromiha MM, and Schomburg D. CUPSAT: prediction of protein stability upon point mutations. *Nucleic Acids Res* 2006;34(Web Server issue):W239-42.
 30. Chen Y, Lu H, Zhang N, Zhu Z, Wang S, Li M. PremPS: Predicting the impact of missense mutations on protein stability. *PLoS Comput Biol* 2020;16(12):100-5.
 31. Frishman D, Argos P. Knowledge-based protein secondary structure assignment. *Proteins* 1995;23(4):566-79.
 32. Aksu G, Genel F, Koturoglu G, Kurugol Z, Kutukculer N. Serum immunoglobulin (IgG, IgM, IgA) and IgG subclass concentrations in healthy children: a study using nephelometric technique. *Turk J Pediatr* 2006;48(1):19-24.
 33. Ozcan E, Rauter I, Garibyan L, Dillon SR, Geha RS. Toll-like receptor 9, transmembrane activator and calcium-modulating cyclophilin ligand interactor, and CD40 synergize in causing B-cell activation. *J Allergy Clin Immunol* 2011;128(3):601-9.
 34. Salzer U, Bacchelli C, Buckridge S, Pan-Hammarstrom Q, Jennings S, Lougaris V, et al. Relevance of biallelic versus monoallelic *TNFRSF13B* mutations in distinguishing disease-causing from risk-increasing *TNFRSF13B* variants in antibody deficiency syndromes. *Blood* 2009;113(9):1967-76.
 35. Liao M, Ye F, Zhang B, Huang L, Xiao Q, Qin M, et al. Genome-wide association study identifies common variants at *TNFRSF13B* associated with IgG level in a healthy Chinese male population. *Genes Immun* 2012;13(6):509-13.
 36. Speletas M, Mamara A, Papadopoulou-Alataki E, Iordanakis G, Liadaki K, Bardaka F, et al. *TNFRSF13B/TACI* alterations in Greek patients with antibody deficiencies. *J Clin Immunol* 2011;31(4):550-9.